J|A|C|S
ARTICLES
Published on Web 06/09/2004

Reaction of the 1,8-Bis(diphenylmethylium)naphthalenediyl Dication with Fluoride: Formation of a Cation Containing a C−F→C Bridge

Huadong Wang, Charles Edwin Webster, Lisa M. Pérez, Michael B. Hall,* and François P. Gabbaï*

Contribution from the Chemistry Department, Texas A&M University, 3255 TAMU, College Station, Texas 77843-3255

Received March 15, 2004; E-mail: gabbai@mail.chem.tamu.edu

Abstract: Treatment of 1,8-bis(diphenylhydroxymethyl)naphthalene with a mixture of $[HBF_4]_{aq}$ and $(CF_3CO)_2O$ affords the corresponding dication, 1,8-bis(diphenylmethylium)naphthalenediyl (**1**$^{2+}$), which was isolated as the $[BF_4]^-$ salt. This dication has been fully characterized, and its structure has been studied computationally. The ^{13}C NMR resonance of the methylium centers appears at 207.7 ppm. As indicated by an X-ray single-crystal analysis, the vicinal methylium centers are separated by 3.112(4) Å. Dication (**1**$^{2+}$) reacts with fluoride to afford [**1**−F]$^+$ which has been isolated as the $[BF_4]^-$ salt. The fluorine atom of [**1**−F]$^+$ is connected to one of the former methylium centers through a typical C−F bond of 1.424(2) Å and forms a long interaction of 2.444(2) Å with the other methylium center. While the structure of [**1**−F]$^+$ can be largely accounted for by considering a simple methylium formulation, density functional calculations followed by an Atom In Molecules analysis as well as a calculation of the Boys localized orbitals indicate that the long C−F interaction of 2.444(2) Å corresponds to a dative bond. Hence, formulation of [**1**−F]$^+$ as an unsymmetrical fluoronium must also be considered. As indicated by ^1H NMR spectroscopy, the structure of this ion is fluxional; the fluorine atom oscillates between the former methylium centers with apparent activation parameters of $\Delta H^{\ddagger} = 52(\pm 3)$ kJ mol^{-1} and $\Delta S^{\ddagger} = -18(\pm 9)$ J K^{-1} mol^{-1} as derived from line shape analysis. This dynamic process, which has also been studied theoretically by B3LYP density functional theory and Møller−Plesset second-order perturbation theory methods, involves symmetrical fluoronium ions as low-energy transition states.

Introduction

Stable triarylmethylium cations[1,2] are the isoelectronic analogues of triarylboranes. Like their boron counterparts, these carbocations constitute powerful Lewis acids which, for example, serve as anionic ligand abstractors for the activation of transition metal olefin polymerization catalysts.[3] A translation of this analogy to the domain of polyfunctional Lewis acids suggests that a new class of polydentate electrophilic host may result from the incorporation of several methylium moieties in a unique molecule.[4−6] For example, it is conceivable that a derivative featuring two methylium moieties connected by a *peri*-substituted naphthalene backbone would display chemistry similar to that of 1,8-bis(boryl)naphthalenes.[7,8] The latter, which have been extensively studied in the context of anion complexation, readily captures fluoride to form a complex featuring a symmetrical B−F−B bridge.[7,9] On the basis of the aforementioned analogy, the formation of a C−F−C bridged species by addition of a fluoride anion to a 1,8-bis(methylium)naphthalenediyl arises as an intriguing possibility (Scheme 1). Similar ideas have been developed by McMurry as well as Sorensen who have demonstrated the formation of a cation featuring a

Scheme 1. Isoelectronic Relationship between 1,8-Bis(boryl)naphthalenes and the Corresponding Dications; Reaction with Fluoride (R = Alkyl or Aryl)

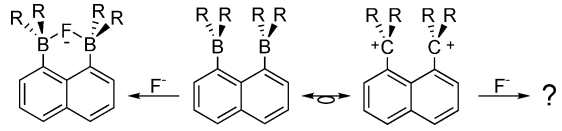

(1) Freedman, H. H. In *Carbonium Ions*; Olah, G. A., Schleyer, P. v. R., Eds.; Wiley-Interscience: New York, 1973; Vol. IV, Chapter 28.
(2) Herse, C.; Bas, D.; Krebs, F. C.; Bürgi, T.; Weber, J.; Wesolowski, T.; Laursen, B. W.; Lacour, J. *Angew. Chem., Int. Ed.* **2003**, *42*, 3162.
(3) For examples, see: (a) Chen, E. Y.-X.; Marks, T. J. *Chem. Rev.* **2000**, *100*, 1391. (b) Piers, W. E.; Irvine, G. J.; Williams, V. C. *Eur. J. Inorg. Chem.* **2000**, 2131.
(4) (a) Hart, H.; Sulzberg, T.; Rafos, R. R. *J. Am. Chem. Soc.* **1963**, *85*, 1800. (b) Volz, H.; Volz de Lecea, M. J. *Tetrahedron Lett.* **1964**, 1871. (c) Hart, H.; Sulzberg, T.; Schwende, Rh.; Young, R. H. *Tetrahedron Lett.* **1967**, 1337.
(5) Prakash, G. K. S.; Rawdah, T. N.; Olah, G. A. *Angew. Chem., Int. Ed. Engl.* **1983**, *22*, 390−401.
(6) For general references on stable carbodications: Reddy, V. P.; Rasul, G.; Prakash, G. K. S.; Olah, G. A. *J. Org. Chem.* **2003**, *68*, 3507. Noack, A.; Schroder, A.; Hartmann, H.; Rohde, D.; Dunsch, L. *Org. Lett.* **2003**, *5*, 2393. Karbach, S.; Vogtle, F. *Chem. Ber.* **1982**, *115*, 427.
(7) (a) Katz, H. E. *J. Org. Chem.* **1985**, *50*, 5027. (b) Katz, H. E. *J. Am. Chem. Soc.* **1986**, *108*, 7640. (c) Solé, S.; Gabbaï, F. P. *Chem. Commun.* **2004**, 1284.
(8) Gabbaï, F. P. *Angew. Chem., Int. Ed.* **2003**, *42*, 2218. Hoefelmeyer, J. D.; Schulte, M.; Tschinkl, M.; Gabbaï, F. P. *Coord. Chem. Rev.* **2002**, *235*, 93.
(9) For related work with 1,2-diborylbenzenes, see: Williams, V. C.; Piers, W. E.; Clegg, W.; Elsegood, M. R. J.; Collins, S.; Marder, T. B. *J. Am. Chem. Soc.* **1999**, *121*, 3244.

C−H−C 3c-2e bond reminiscent of the ubiquitous 3c-2e B−H−B linkages.[10,11]

Formally, a species featuring a C−F−C bridge corresponds to a fluoronium cation whose existence, in the condensed state, remains to be confirmed. Indeed, we note that while halonium ions of the type $[R_3C-X-CR_3]^+$ (X = halogen, R = alkyl or aryl) are known for chlorine, bromine, and iodine,[12,13] the corresponding fluorine species are remarkably elusive and have not been isolated nor structurally characterized.[14] In comparison to its heavier group 17 congeners, fluorine possesses the highest one-electron ionization energies for the outer-shell s and p orbitals.[15] These intrinsic characteristics are responsible for the high electronegativity of fluorine and also provide a rationale for the reluctance of this element to form fluoronium ions. Although the latter can be observed as gas-phase species,[16−19] the mere intermediacy of fluoronium ions in the condensed state has long been questioned[20] and often refuted.[12,21] Recent studies, however, provide strong support for the intermediacy of such cations in intramolecular fluorine transfer reactions.[22,23]

As part of our interest in the chemistry of polydentate Lewis acids, we have recently focused on the synthesis of 1,8-bis-(methylium)naphthalenediyl dications.[24] Using some of the elegant strategies developed for the synthesis of dications featuring a biphenyl or binaphthyl backbone,[4c,25−27] we prepared 1,8-bis(bis(*p*-methoxyphenyl)methylium)naphthalenediyl,[24] a dication in which the diarylmethylium centers are stabilized by electron donor *p*-methoxy groups. In an extension of this chemistry, we would like to describe the unsubstituted 1,8-bis-(diphenylmethylium)naphthalenediyl dication ($\mathbf{1}^{2+}$). This dication reacts with fluoride to afford a monocation ($[\mathbf{1}-F]^+$) which possesses a bridging fluorine atom preferentially bound to one of the two former methylium centers.

Table 1. Crystallographic Data

	$[\mathbf{1}]^{2+}[BF_4]^-_2$	$[\mathbf{1}-F]^+[BF_4]^-$
formula	$C_{36}H_{26}B_2F_8$	$C_{36}H_{26}BF_5$
M_r	632.19	564.38
cryst syst	monoclinic	triclinic
space group	$P2_1/c$	$P\bar{1}$
a (Å)	17.6581(15)	10.190(2)
b (Å)	10.4884(9)	10.273(2)
c (Å)	16.0575(13)	14.506(3)
α (deg)		110.71(3)
β (deg)	104.633(2)	104.54(3)
γ (deg)		95.19(3)
V (Å^3)	2877.5(4)	1347.7(5)
ρ_{calcd} (g cm^{-3})	1.459	1.391
Z	4	2
F(000) (e)	1296	584
μ(Mo Kα) (mm^{-1})	0.119	0.103
absorption correction	empirical	
T_{min}/T_{max}	0.4727/0.7781	
T (K)	110(2)	110(2)
θ range (deg)	1.19−23.99	2.11−23.29
scan mode	ω	ω
no. of rflns measd	13 439	5824
no. of unique rflns (R_{int})	4501 (0.0324)	3860
no. of refined params	466	379
R1, wR2 ($I > 2\sigma(I)$)	0.0622, 0.1456	0.0325, 0.0821

Scheme 2 [a]

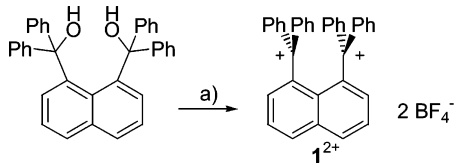

[a] (a) $[HBF_4]_{aq}/(CF_3CO)_2O$, 25 °C.

Experimental Section

General Considerations. 1,8-Bis(diphenylhydroxymethyl)naphthalene was synthesized by following a published procedure.[28] $[(Me_2N)_3S]^+[Me_3SiF_2]^-$ was purchased from Aldrich and used without purification. Solvents were dried by reflux under N_2 over the appropriate drying agents and freshly distilled prior to use. Acetonitrile and chloroform were dried over CaH_2. Diethyl ether and THF were dried over Na/K. Air-sensitive compounds were handled under a N_2 atmosphere using standard Schlenk and glovebox techniques. Elemental analyses were performed at Atlantic Microlab (Norcross, GA). All melting points were measured on samples in sealed capillaries and are uncorrected. NMR spectra were recorded on Varian Unity Inova 400 FT NMR (399.63 MHz for ^{1}H 376.03 MHz for ^{19}F 100.50 MHz for ^{13}C) and Varian Inova 500 FT NMR (500.62 MHz for ^{1}H 125.89 MHz for ^{13}C) spectrometers. Chemical shifts δ are given in ppm and are referenced against external Me_4Si (^{1}H, ^{13}C) and $CFCl_3$ (^{19}F).

Synthesis of $[\mathbf{1}]^{2+}[\mathbf{BF_4}]_2^-$. To a suspension of 1,8-bis(diphenylhydroxymethyl)naphthalene (0.83 g, 1.7 mmol) in trifluoroacetic anhydride (10 mL) was added 48% HBF_4 (1.0 mL, 7.7 mmol). After the mixture was stirred for 2 h, ether (30 mL) was added to the mixture which resulted in the precipitation of $[\mathbf{1}]^{2+}[BF_4]^-_2$ as a dark-red solid. This solid was isolated by filtration, washed with ether, and dried in a vacuum (1.0 g, yield 94%). Single crystals of this salt were obtained by vapor diffusion of diethyl ether into a solution of acetonitrile. ^{1}H

(10) McMurry, J. E.; Lectka, T. *Acc. Chem. Res.* **1992**, *25*, 47. McMurry, J. E.; Lectka, T.; Hodge, C. N. *J. Am. Chem. Soc.* **1989**, *111*, 8867. Taeschler, C.; Parvez, M.; Sorensen, T. S. *J. Phys. Org. Chem.* **2002**, *15*, 36.
(11) Hoffmann, R.; Tantillo, D. J. *Angew. Chem., Int. Ed.* **2003**, *42*, 5877. Tantillo, D. J.; Hoffmann, R. *J. Am. Chem. Soc.* **2003**, *125*, 4042.
(12) Olah, G. A. *Halonium Ions*; Wiley: New York, 1975. Olah, G. A.; Prakash, G. K. S.; Sommer, J. *Superacids*; John Wiley & Sons: New York, 1985. Olah, G. A.; DeMember, J. R.; Mo, Y. K.; Svoboda, J. J.; Schilling, P. Olah, J. A. *J. Am. Chem. Soc.* **1974**, *96*, 884.
(13) Rathore, R.; Lindeman, S. V.; Zhu, C.-J.; Mori, T.; Schleyer, P. v. R.; Kochi, J. K. *J. Org. Chem.* **2002**, *67*, 5106.
(14) Olah, G. A.; Rasul, G.; Hachoumy, M.; Burrichter, A.; Prakash, G. K. S. *J. Am. Chem. Soc.* **2000**, *122*, 2737.
(15) Allen, L. C. *J. Am. Chem. Soc.* **1989**, *111*, 9003.
(16) Beauchamp, J. L.; Holtz, D.; Woodgate, S. D.; Patt, S. L. *J. Am. Chem. Soc.* **1972**, *94*, 2798.
(17) Viet, N.; Cheng, X.; Morton, T. H. *J. Am. Chem. Soc.* **1992**, *114*, 7127. Nguyen, V.; Mayer, P. S.; Morton, T. H. *J. Org. Chem.* **2000**, *65*, 8032. Leblanc, D.; Kong, J.; Mayer, P. S.; Morton, T. H. *Int. J. Mass Spectrom.* **2003**, *222*, 451.
(18) Nichols, L. S.; McKee, M. L.; Illies, A. J. *J. Am. Chem. Soc.* **1998**, *120*, 1538−1544. Chiavarino, B.; Crestoni, M. E.; Fornarini, S.; Kuck, D. *J. Phys. Chem. A* **2003**, *107*, 4619.
(19) Renzi, G.; Roselli, G.; Grandinetti, F.; Filippi, A.; Speranza, M. *Angew. Chem., Int. Ed.* **2000**, *39*, 1673. Speranza, M.; Angelini, G. *J. Am. Chem. Soc.* **1980**, *102*, 3115.
(20) Peterson, P. E.; Bopp, R. J. *J. Am. Chem. Soc.* **1967**, *89*, 1283. Clark, D. T. *Special Lectures of the XXIII International Congress of Pure and Applied Chemistry*, Boston; Butterworth: London, 1971; Vol. I, p 31.
(21) Olah, G. A.; Prakash, G. K. S.; Krishnamurthy, V. V. *J. Org. Chem.* **1983**, *48*, 5116.
(22) Ferraris, D.; Cox, C.; Anand, R.; Lectka, T. *J. Am. Chem. Soc.* **1997**, *119*, 4319.
(23) For related work regarding the generation of diarylfluoronium by radiochemical methods, see: Shchepina, N. E.; Nefedov, V. D.; Toropova, M. A.; Badun, G. A.; Fedoseev, V. M.; Avrorin, V. V. *Radiochemistry* **2001**, *43*, 525. Shchepina, N. E.; Nefedov, V. D.; Toropova, M. A.; Badun, G. A.; Avrorin, V. V.; Fedoseev, V. M. *Radiochemistry* **2002**, *44*, 378. Shchepina, N. E.; Badun, G. A.; Nefedov, V. D.; Toropova, M. A.; Fedoseev, V. M.; Avrorin, V. V.; Lewis, S. B. *Tetrahedron Lett.* **2002**, *43*, 4123.
(24) Wang, H.; Gabbaï, F. P. *Angew. Chem., Int. Ed.* **2004**, *43*, 184.
(25) (a) Suzuki, T.; Nishida, J.; Tsuji, T. *Angew. Chem., Int. Ed. Engl.* **1997**, *36*, 1329. (b) Suzuki, T.; Nishida, J.; Tsuji, T. *J. Chem. Soc., Chem. Commun.* **1998**, 2193.
(26) Carey, K. A.; Clegg, W.; Elsegood, M. R. J.; Golding, B. T.; Hill, M. N. S.; Maskill, H. *J. Chem. Soc., Perkin Trans. 1* **2002**, 2673.
(27) (a) Nishida, J.; Suzuki, T.; Ohkita, M.; Tsuji, T. *Angew. Chem., Int. Ed.* **2001**, *40*, 3251. (b) Higuchi, H.; Ohta, E.; Kawai, H.; Fujiwara, K.; Tsuji, T.; Suzuki, T. *J. Org. Chem.* **2003**, *68*, 6605.
(28) Letsinger, R. L.; Gilpin, J. A.; Vullo, W. J. *J. Org. Chem.* **1962**, *27*, 672.

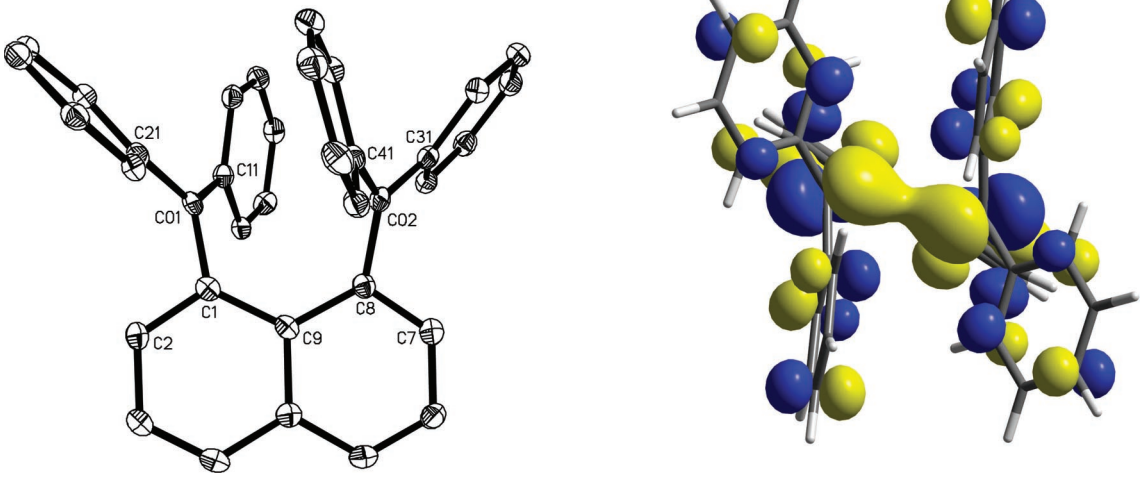

Figure 1. Left: ORTEP plot of the molecular structure of $\mathbf{1}^{2+}$ in $[\mathbf{1}^{2+}][BF_4^-]_2$ with thermal ellipsoids set at the 50% probability level. Hydrogen atoms are omitted for clarity. Selected bond lengths (in Å) and bond angles (in deg) (as compared to calculated values in brackets): C(01)−C(11) 1.433(4) [1.455], C(01)−C(21) 1.438(4) [1.445], C(01)−C(1) 1.474(4) [1.467], C(01)−C(02) 3.112(4) [3.231], C(02)−C(31) 1.436(4), C(02)−C(41) 1.449(4), C(02)−C(8) 1.460(4), C(11)−C(01)−C(21) 123.5(2) [120.3], C(11)−C(01)−C(1) 119.6(2) [120.1], C(21)−C(01)−C(1) 116.7(2) [119.1], C(31)−C(02)−C(41) 120.1(2), C(31)−C(02)−C(8) 120.3(2), C(41)−C(02)−C(8) 119.1(2). Right: The LUMO (at 0.015 isodensity value) of B3LYP optimized $\mathbf{1}^{2+}$ viewed from the top of the molecule.[38]

NMR (CD_3CN, 500 MHz): δ 6.59 (br, 2H, C_6H_5), 6.78 (br, 2H, C_6H_5), 7.41 (br, 2H, C_6H_5), 7.48−7.71 (m, 4H, C_6H_5), 7.54 (d, J = 7.8 Hz, 4H, C_6H_5), 7.62 (d, J = 7.4 Hz, 2H, H_{naph}), 7.80 (br, 2H, C_6H_5), 8.02 (br, 2H, C_6H_5), 8.10 (pseudo t, J = 7.6 Hz, 2H, H_{naph}), 8.27 (br, 2H, C_6H_5), 9.01 (d, J = 8.1 Hz, 2H, H_{naph}). ^{13}C NMR (CD_3CN, 125.9 MHz): δ 128.0, 129.6, 130.0, 131.9, 132.7, 136.6, 137.4, 139.0, 139.6, 139.8, 142.6, 143.5, 144.7, 147.0, 150.9, 207.7. Anal. Calcd for $C_{36}H_{26}B_2F_8$: C, 68.33; H, 4.14. Found: C, 68.29; H, 4.17.

Synthesis of $[\mathbf{1}-F]^+[BF_4]^-$. An acetonitrile solution (5 mL) of $[(Me_2N)_3S]^+[Me_3SiF_2]^-$ (0.40 g, 1.45 mmol) was added to a solution of $[\mathbf{1}]^{2+}[BF_4]^-_2$ (0.40 g, 0.63 mmol) in acetonitrile (10 mL). After the mixture was stirred for 1 h, the solvent was evaporated under vacuum. The purple residue was washed with THF (5 mL) and identified as a mixture of $[\mathbf{1}-F]^+[BF_4]^-$ (NMR yield 17%) and $[(Me_2N)_3S]^+[BF_4]^-$. Single crystals of $[\mathbf{1}-F]^+[BF_4]^-$ suitable for X-ray structural analysis were obtained by vapor diffusion of diethyl ether into an acetonitrile solution. ^{1}H NMR ($CDCl_3$, 400 MHz, −60 °C): δ 6.02 (d, J = 7.7 Hz, 1H, C_6H_5), 6.58 (d, J = 7.1 Hz, 2H, C_6H_5), 6.75 (m, 3H, C_6H_5), 6.92−7.25 (m, 9H, $H_{aromatic}$), 7.42−7.52 (m, 2H, $H_{aromatic}$), 7.55 (pseudo t, J = 7.5 Hz, 1H, C_6H_5), 7.64 (pseudo t, J = 7.9 Hz, 1H, H_{naph}), 7.74−7.83 (m, 2H, $H_{aromatic}$), 7.95 (pseudo t, J = 7.6 Hz, 1H, C_6H_5), 8.14 (d, J = 7.7 Hz, 1H, H_{naph}), 8.21 (pseudo t, J = 7.5 Hz, 1H, C_6H_5), 8.32 (d, J = 7.4 Hz, 1H, C_6H_5), 8.59 (d, J = 8.0 Hz, 1H, H_{naph}). ^{13}C NMR ($CDCl_3$, 100.5 MHz, −60 °C): δ 105.1 (d, J = 178.5 Hz), 124.4, 126.7, 126.9, 127.1, 127.6, 127.8, 127.9, 128.2, 128.9, 129.2, 129.4, 130.0, 130.1, 130.7, 130.9, 134.6, 135.4, 135.6, 135.8, 136.2, 137.6, 138.8, 139.9, 140.9, 141.3, 141.4, 141.7, 142.3, 143.2, 144.9, 146.1, 146.4, 209.3 (d, J = 11.8 Hz).

Crystallography. The crystallographic measurements were performed using a Siemens SMART-CCD area detector diffractometer, with graphite-monochromated Mo Kα radiation (λ = 0.710 69 Å). Specimens of suitable size and quality were selected and mounted onto glass fibers with Apiezon grease. The structures were solved by direct methods, which successfully located most of the non-hydrogen atoms. Subsequent refinement on F^2 using the SHELXTL/PC package (version 5.1) allowed for the location of the remaining non-hydrogen atoms. Further crystallographic details can be found in Table 1.

Exchange Rate Constants k for $[\mathbf{1}-F]^+$ in $CDCl_3$. VT ^{1}H NMR data were recorded on the Varian Unity Inova 400 FT NMR spectrometer. The line shape of the CH_{naph} resonances was analyzed using the gNMR program (Version 5). The resulting rates were fit to the Eyring equation which yielded apparent values for $\Delta H^{\ddagger}$ and $\Delta S^{\ddagger}$.

Theoretical Calculations. The theoretical calculations have been carried out with the Gaussian 98[29] implementations of second-order Møller−Plesset[30] (MP2) perturbation theory and of B3LYP [Becke three-parameter exchange functional (B3)[31] and the Lee−Yang−Parr correlation functional (LYP)[32]] density functional theory (DFT).[33] All ab initio and DFT calculations used the default SCF convergence for geometry optimizations (10^{-8}). All DFT calculations used the default pruned fine grids for energies (75 302) and default pruned course grids for gradients and Hessians (35 110). The 6-31G+(d) basis sets of Pople and co-workers[34] were used for the fluorine and methylium carbon atoms, and the 6-31G basis sets were used for all other carbon and all hydrogen. Polarization d functions used spherical harmonic representations. All structures were fully optimized, and analytical frequency calculations were performed on all structures (except MP2 optimized structures) to ensure either a minimum or a first-order saddle point was achieved. All reported relative energies are enthalpies ($\Delta H°$ or $\Delta H^{\ddagger}$), reported for standard conditions, 298 K and 1 atm. Because of the number of atoms in these particular compounds, MP2 frequency calculations are beyond the capabilities of most current ab initio codes. Therefore, relative MP2 enthalpies use electronic energies from optimized MP2 geometries with vibrational and thermodynamic corrections from B3LYP frequency calculations at B3LYP optimized

(29) Frisch, M. J.; Trucks, G. W.; Schlegel, H. B.; Scuseria, G. E.; Robb, M. A.; Cheeseman, J. R.; Zakrzewski, V. G.; Montgomery, J. A.; Stratmann, R. E.; Burant, J. C.; Dapprich, S.; Millam, J. M.; Daniels, A. D.; Kudin, K. N.; Strain, M. C.; Farkas, O.; Tomasi, J.; Barone, V.; Cossi, M.; Cammi, R.; Mennucci, B.; Pomelli, C.; Adamo, C.; Clifford, S.; Ochterski, J.; Petersson, G. A.; Ayala, P. Y.; Cui, Q.; Morokuma, K.; Malick, D. K.; Rabuck, A. D.; Raghavachari, K.; Foresman, J. B.; Cioslowski, J.; Ortiz, J. V.; Stefanov, B. B.; Liu, G.; Liashenko, A.; Piskorz, P.; Komaromi, I.; Gomperts, R.; Martin, R. L.; Fox, D. J.; Keith, T.; Al-Laham, M. A.; Peng, C. Y.; Nanayakkara, A.; Gonzalez, C.; Challacombe, M.; Gill, P. M. W.; Johnson, B.; Chen, W.; Wong, M. W.; Andres, J. L.; Gonzalez, A. C.; Head-Gordon, M.; Replogle, E. S.; Pople, J. A. *Gaussian 98*, revision A.11.3; Gaussian, Inc.: Pittsburgh, PA, 1998.
(30) Møller, C.; Plesset, M. S. *Phys. Rev.* **1934**, *46*, 618.
(31) Becke, A. D. *J. Chem. Phys.* **1993**, *98*, 5648.
(32) Lee, C.; Yang, W.; Parr, R. G. *Phys. Rev. B* **1988**, *37*, 785.
(33) Parr, R. G.; Yang, W. *Density Functional Theory of Atoms and Molecules*; Oxford University Press: New York, 1989.
(34) Ditchfield, R.; Hehre, W. J.; Pople, J. A. *J. Chem. Phys.* **1971**, *54*, 724. Hehre, W. J.; Ditchfield, R.; Pople, J. A. *J. Chem. Phys.* **1972**, *56*, 2257. Hariharan, P. C.; Pople, J. A. *Theor. Chim. Acta* **1973**, *28*, 213. Francl, M. M.; Pietro, W. J.; Hehre, W. J.; Binkley, J. S.; Gordon, M. S.; DeFrees, D. J.; Pople, J. A. *J. Chem. Phys.* **1982**, *77*, 3654.

geometries. This approximation should be reasonably accurate because the MP2 optimized geometries are very similar to the B3LYP optimized geometries.

Results and Discussions

Synthesis and Characterization of 1,8-Bis(diphenylmethylium)naphthalenediyl Bis(tetrafluoroborate) ([1]$^{2+}$[BF$_4$]$^-_2$). Applying the strategy recently utilized for the synthesis of 1,8-bis(bis(*p*-methoxyphenyl)methylium)naphthalenediyl dication,[24] we found that the simple treatment of the known 1,8-bis(diphenylhydroxymethyl)naphthalene[28] with a mixture of [HBF$_4$]$_{aq}$ and (CF$_3$CO)$_2$O affords the corresponding dication, 1,8-bis(diphenylmethylium)naphthalenediyl (**1**$^{2+}$), which was isolated as the [BF$_4$]$^-$ salt (Scheme 2). This dication, which can be regarded as a fused version of the triphenylmethylium (trityl) cation, has been fully characterized. The ^{1}H NMR spectrum of **1**$^{2+}$ features the expected signals for a symmetrically *peri*-substituted naphthalene derivative with the hydrogen atoms at the 2- and 7-positions shifted downfield by 1.32 ppm with respect to the diol. The ^{13}C resonance of the carbocationic centers appears at 207.7 ppm which is comparable to that observed for the trityl cation.[35] As indicated by a single-crystal X-ray analysis (Figure 1, Table 1),[36] the steric crowding present in this dication leads to distortions of the C(9)−C(8)−C(02) (125.7(3)°) and C(9)−C(1)−C(01) (125.5(2)°) angles which are larger than the ideal value of 120°. As indicated by the sum of the bond angles at C(01) ($\Sigma_{(C-C(01)-C)}$ = 359.8°) and C(02) ($\Sigma_{(C-C(02)-C)}$ = 359.5°), each methylium center adopts a trigonal planar arrangement in agreement with a sp^2 hybridization. Finally, the vicinal methylium centers are separated by 3.112(4) Å. This distance is larger than that observed in the *p*-methoxy-substituted analogue of **1**$^{2+}$, 1,8-bis(bis(*p*-methoxyphenyl)-methylium)naphthalenediyl, in which the methylium centers are separated by 3.076(2) Å. The larger separation observed in **1**$^{2+}$ possibly results from increased electrostatic repulsions between the methylium center which, in the absence of electron donor substituent, bear a larger portion of the cationic charges. Recognizing the isolobal relationship that exists between a Ph$_3$B and a Ph$_3$C$^+$ fragment, **1**$^{2+}$ is structurally and electronically similar to 1,8-bis(diphenylboryl)naphthalene which features an interboron separation of 3.002(2) Å.[37]

The B3LYP optimized geometry of this dication is close to that observed for the dication in [**1**]$^{2+}$[BF$_4$]$^-_2$ (Figure 1). An examination of the B3LYP orbitals reveals that the empty methylium p orbitals largely contribute to the LUMO and are oriented toward one another in a transannular fashion. Hence, it can be expected that the two methylium centers are the most electrophilic site of the molecule.

Reaction of 1,8-Bis(diphenylmethylium)naphthalenediyl (1^{2+}) with Fluoride. Addition of 1 or preferably 2 equiv of [Me$_3$SiF$_2$]$^-$[S(NMe$_2$)$_3$]$^+$ to a solution of [**1**]$^{2+}$[BF$_4$]$^-_2$ in acetonitrile results in the formation of [**1**−F]$^+$[BF$_4$]$^-$ which could be recrystallized by diffusion of ether vapors (Scheme 3). The use of 2 equiv of [Me$_3$SiF$_2$]$^-$[S(NMe$_2$)$_3$]$^+$ did not afford the difluoride **1**−F$_2$ but instead led to a higher yield of [**1**−F]$^+$-[BF$_4$]$^-$. Crystals of [**1**−F]$^+$[BF$_4$]$^-$ have a deep purple color and are very air-sensitive. As indicated by a single-crystal X-ray analysis (Figure 2, Table 1), the [**1**−F]$^+$ and [BF$_4$]$^-$ ions are well separated. The cation [**1**−F]$^+$ is C_1 symmetrical, with the bridging fluorine atom preferentially bound to one of the two former methylium centers (Figures 2 and 3). Indeed, inspection of the structure shows that the C(01) carbon center is tetrahedral and forms a regular C−F bond of 1.424(2) Å with the bridging fluorine atom.[39] By contrast, the C(02) carbon atom retains a formal sp^2 hybridization ($\Sigma_{(C-C(02)-C)}$ = 359.5°) and forms a contact of 2.444(2) Å with the bridging fluoride atom. While the C(02)−F linkage is markedly longer than the C(01)−F single bond, it remains less than the sum of the van der Waals radii of the two elements (r_{vdw}(F) = 1.30−1.38 Å, r_{vdw}(C) = 1.7 Å).[40] Moreover, the C(01)−F−C(02) angle is 111.11(9)°, a value expected for a formally sp^3 hybridized fluorine atom with one of its lone pairs pointing directly toward the C(02) center (Figure 2). In agreement with this view, the C(31)−C(02)−F (90.4(1)°),

Scheme 3 [a]

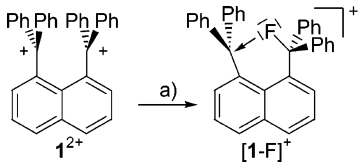

[a] (a) [Me$_3$SiF$_2$]$^-$[S(NMe$_2$)$_3$]$^+$, MeCN, 25 °C.

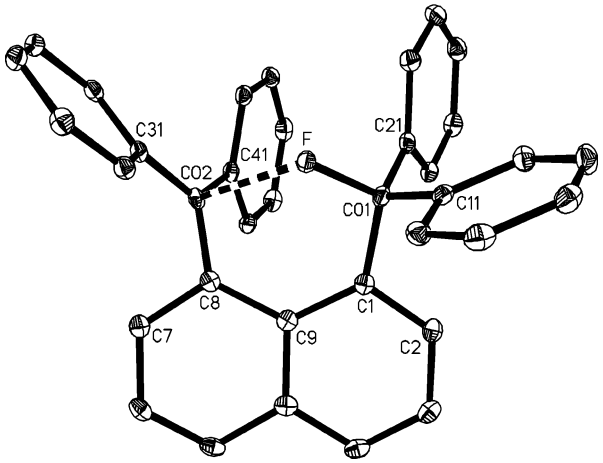

Figure 2. Crystal structure of [**1**−F$^+$] in [**1**−F$^+$][BF$_4^-$] with thermal ellipsoids set at the 50% probability level. Hydrogen atoms are omitted for clarity. Selected bond lengths (Å) and bond angles (deg): F−C(01) 1.4243(17), F−C(02) 2.4444(17), C(01)−C(21) 1.522(2), C(01)−C(11) 1.535(2), C(01)−C(1) 1.537(2), C(01)−C(02) 3.242(2), C(02)−C(31) 1.438(2), C(02)−C(41) 1.446(2), C(02)−C(8) 1.460(2), C(01)−F−C(02) 111.11(9), F−C(01)−C(21) 106.63(12), F−C(01)−C(11) 103.91(11), C(21)−C(01)−C(11) 112.80(13), F−C(01)−C(1) 108.20(12), C(21)−C(01)−C(1) 115.17(13), C(11)−C(01)−C(1) 109.37(12), F−C(01)−C(02) 44.70(7), C(21)−C(01)−C(02) 95.04(10), C(11)−C(01)−C(02) 144.53(10), C(1)−C(01)−C(02) 75.16(9), C(31)−C(02)−C(41) 122.92(14), C(31)−C(02)−C(8) 117.99(14), C(41)−C(02)−C(8) 118.59(13), C(31)−C(02)−F 90.40(10), C(41)−C(02)−F 99.58(10), C(8)−C(02)−F 86.73(9).

(35) Arentt, E. M.; Flowers, R. A., II; Ludwig, R. T.; Meekhof, A. E.; Walek, S. A. *J. Phys. Org. Chem.* **1997**, *10*, 499.
(36) X-ray data have been deposited at the Cambridge Crystallographic Data Centre and allocated the deposition numbers CCDC 229338 & 229339.
(37) Hoefelmeyer, J. D.; Gabbaï, F. P. *J. Am. Chem. Soc.* **2000**, *122*, 9054. Hoefelmeyer, J. D.; Schulte, M.; Tschinkl, M.; Gabbai, F. P. *Coord. Chem. Rev.* **2002**, *235*, 93.
(38) An in-house Cerius^2 SDK implementation of an interface between Cerius^2 and POV-Ray 3.1 written by J. Manson was used in the production of Figures 1, 3, 4, and 6. Cerius^2 4.8: Accelrys Inc., 9685 Scranton Road, San Diego, CA 92121-3752, USA; http://www.accelrys.com/; POV-Ray: POV-Team co/ Hallam Oaks P/L, P.O. Box 407, Williamstown, Victoria, 3016, Australia; http://www.povray.org.
(39) The C−F bond length in Ph$_3$CF is 1.48 Å. See: Takusagawa, F.; Jacobson, R. A.; Trahanovsky, W. S.; Robbins, M. D. *Cryst. Struct. Commun.* **1976**, *5*, 753.
(40) Nyburg, S. C.; Faerman, C. H. *Acta Crystallogr., Sect. B* **1985**, *41*, 274. Caillet, J.; Claverie, P. *Acta Crystallogr.* **1975**, *A31*, 448.

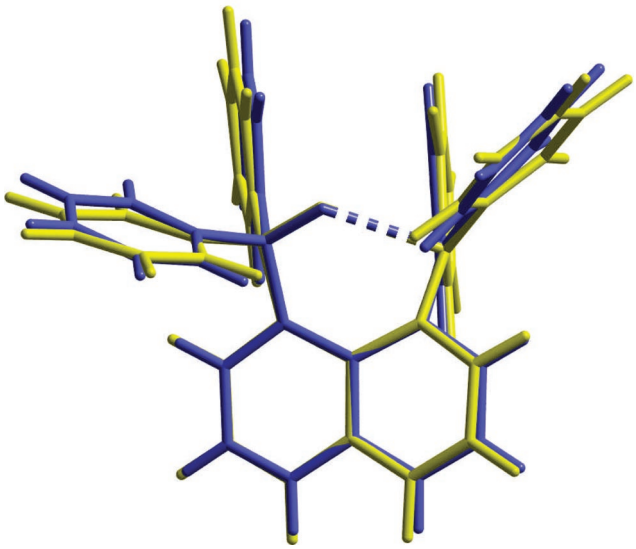

Figure 3. An overlay of the experimental (blue) and calculated (yellow) structures of $[\mathbf{1}-F]^+$ viewed parallel to the naphthalene ring.

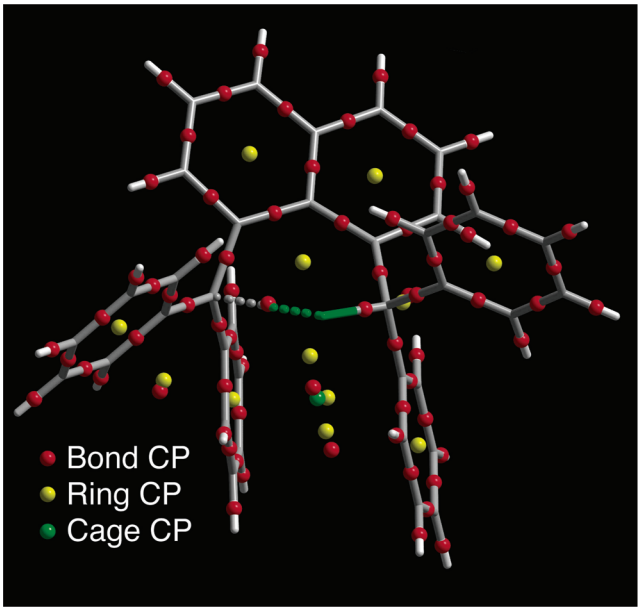

Figure 4. DFT optimized structure of $[\mathbf{1}-F]^+$ showing the critical points (CP) derived from the Atoms In Molecules (AIM) analysis. There are 73 bond CP's, each of which corresponds to a minimum in the electron density $\rho(r)$ along the path connecting bonded atoms and a maximum in $\rho(r)$ in the two directions orthogonal to the bond path; there is a bond CP between each methylium carbon C(01) and C(02) and the fluorine. There are 12 ring CP's (yellow) which occur where $\rho(r)$ is a minimum in the plane within the ring of bonded atoms, and there is one cage CP (light green) which corresponds to a local minimum of $\rho(r)$.[38]

C(41)−C(02)−F (99.6(1)°), and C(8)−C(02)−F (86.7(1)°) angles are close to 90°, which indicates that the fluorine atom is positioned along the direction of the p-orbital of the C(02) carbon center.

$[\mathbf{1}-F]^+$ and other stationary points on the potential energy surface (PES) (vide infra) of this cation were optimized using B3LYP-DFT and ab initio MP2.[41] The lowest energy structure of the ion has C_1 symmetry, $[\mathbf{1}-F]^+$, and corresponds very closely to the experimental geometry determined by single-crystal X-ray diffraction (Figure 3 and Table 2). Significantly, the calculated bond distances and angles involving the bridging fluorine atom are remarkably close to those determined experimentally (Table 2).

To elucidate the nature of the bonding interactions involving the unsymmetrically coordinated fluorine atom, an Atoms In Molecules (AIM) analysis[42] was performed with AIM2000[43] on the density of the optimized geometry of the C_1 minimum. The AIM analysis[44] indicates bond paths and bond critical points (CP) between the fluorine atom F and both central carbon atoms C(01) and C(02) (Figure 4). Thus, this robust analysis confirms the bonding nature of both the C(01)−F and the C(02)−F interactions. The C(01)−F bond is strong and very covalent as indicated by the larger value of the electron density ($\rho(r) = 2.09 \times 10^{-1}$ e bohr^{-3}) and the Laplacian value ($-\frac{1}{4}\nabla^2\rho(r) = 3.64 \times 10^{-2}$ e bohr^{-5}) at the bond CP (Figure 5).[42] In comparison, the C(02)−F bond is weaker and more dative as indicated by the smaller value of the electron density ($\rho(r) = 2.16 \times 10^{-2}$ e bohr^{-3}) and the Laplacian value ($-\frac{1}{4}\nabla^2\rho(r) = -1.93 \times 10^{-2}$ e bohr^{-5}) at the bond CP.[42] The 2-D plots of the density and the Laplacian in the plane of C(01), F, and C(02) are shown in Figure 5. With the characteristic electron concentration at the C(01) and F centers as well as along the line connecting these two atoms, the Laplacian plot illustrates the covalent nature of the short C(01)−F linkage. From the same plot, the C(02)−F interaction appears to be dative in character. Indeed, a region of electron concentration located on F points toward the empty p-orbital of the C(02) center. The presence of this empty p-orbital is indicated by a depletion of the electron density at C(02). Further evidence of the delocalized

Table 2. Experimental and Calculated Bond Distances (Å) and Angles (deg)

	$[\mathbf{1}-F]^+$ (X-ray)	$[\mathbf{1}-F]^+$ (B3LYP)	$[\mathbf{2}-F]^+$ (B3LYP)	$[C_2\text{–}\mathbf{TS}\text{–}F]^+$ (B3LYP)	$[C_s\text{–}\mathbf{TS}\text{–}F]^+$ (B3LYP)	$[\mathbf{TS}_{1-2}\text{–}F]^+$ (B3LYP)
C01−F	1.424(2)	1.437	1.441	1.763	1.752	1.434
C02−F	2.444(2)	2.468	2.434	1.763	1.752	2.429
C01−F−C02	111.11(9)	113.9	118.5	126.3	124.6	119.8
C31−C02−F	90.4(1)	94.7	86.3	98.2	98.3	97.9
C41−C02−F	99.6(1)	97.9	99.4	100.4	102.5	91.2
C8−C02−F	86.7(1)	85.3	92.6	101.9	101.1	88.7

	$[\mathbf{1}-F]^+$ (MP2)	$[\mathbf{2}-F]^+$ (MP2)	$[C_2\text{–}\mathbf{TS}\text{–}F]^+$ (MP2)	$[C_s\text{–}\mathbf{TS}\text{–}F]^+$ (MP2)	$[\mathbf{TS}_{1-2}\text{–}F]^+$ (MP2)
C01−F	1.446	1.451	1.723	1.714	1.443
C02−F	2.410	2.414	1.723	1.714	2.359
C01−F−C02	112.0	113.8	125.3	122.7	118.9
C31−C02−F	93.4	102.8	99.6	99.1	95.9
C41−C02−F	96.7	97.8	97.6	81.9	90.4
C8−C02−F	85.1	101.5	102.7	95.4	88.9

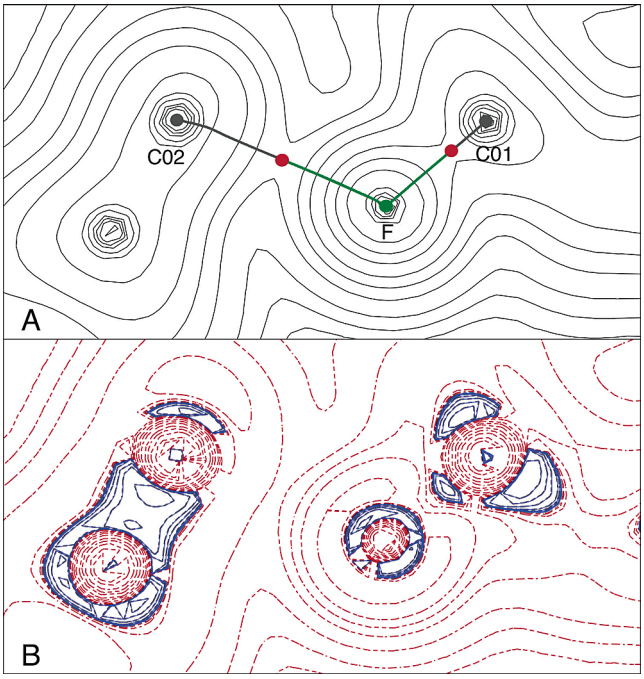

Figure 5. (A) Contour plot of the electron density of $[\mathbf{1}-F]^+$ in the C(02)−F−C(01) plane. The contours are $2^n \times 10^m$ ($n = 1, 2, 3$) and range from 0.002 to 20. The plane was selected to contain the carbon atomic CP, gray circles; fluorine atomic CP, green circle; and bond CP, red circles. The gradient paths connecting the bond critical points to their respective atomic critical points are illustrated as gray and green lines. (B) Contour plot of $-{}^1/_4\nabla^2\rho(r)$ for $[\mathbf{1}-F]^+$ in the same plane illustrating the covalent nature of the short C−F bond and the dative nature of the long C−F bond. The positive contours (solid blue) are $2^n \times 10^m$ ($n = 1, 2, 3$) and range from 0.002 to 2. The negative contours (dashed red) are $-(2^n) \times 10^m$ ($n = 1, 2, 3$) and range from −0.002 to −800.

electron sharing between F and C(02) is shown by the Boys localized orbital[45] (Figure 6) which corresponds to this interaction. The lone pair of the F atom is clearly extended in the direction of C(02) and mixes with the p-orbital of this carbon atom to form a dative bond. The collective evidence about the long C(02)−F interaction supports that this linkage involves electron sharing rather than a purely electrostatic interaction.

In agreement with its bridging location, the ^{19}F NMR resonance of the bridging fluorine atom in $[\mathbf{1}-F]^+$ (−117.0 ppm at 25 °C in CD_3CN) appears downfield from that of Ph_3CF (−126.7 ppm at 25 °C in CD_2Cl_2).[46] The low-temperature carbon spectrum of $[\mathbf{1}-F]^+$ at −60°C in $CHCl_3$ indicates that the fluorine bridge remains unsymmetrical in solution at this temperature. Indeed, two distinct ^{13}C NMR signals are detected for the former methylium centers of $\mathbf{1}^{2+}$. The resonances of the C(01) (105.1 ppm, $J_{CF} = 178.5$ Hz) and C(02) (209.3 ppm, $J_{CF} = 11.8$ Hz) centers both appear as a doublet. While the chemical shift of the C(02) resonance indicates that this atom retains considerable methylium character, the magnitude of the coupling

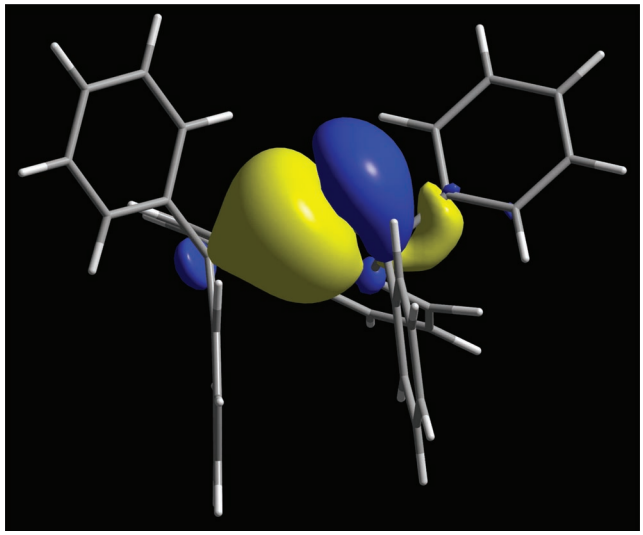

Figure 6. Boys localized orbital (at 0.01 isodensity value) in $[\mathbf{1}-F]^+$ showing the delocalization of the F 2p "lone pair" on the methylium C(02) atom (viewed perpendicular to the naphthalene ring).[38]

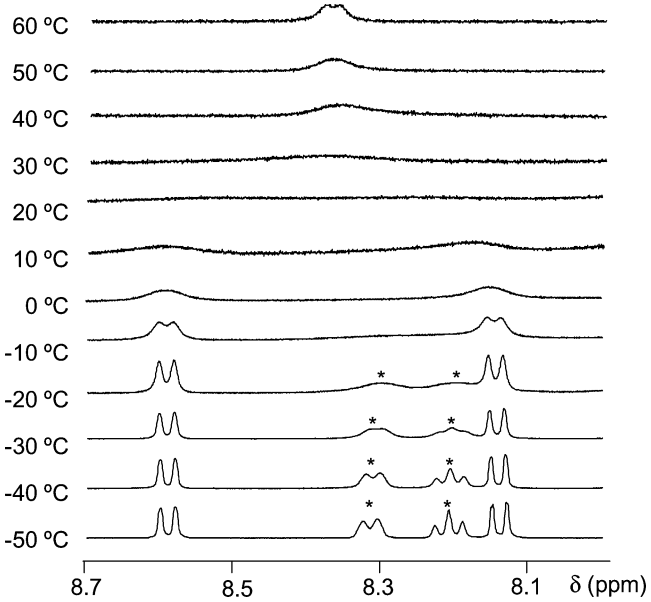

Figure 7. Variable ^1H NMR spectrum of $[\mathbf{1}-F]^+$ in $CDCl_3$. Portion of the spectrum showing the 2- and 7-$CH_{naphthalene}$ resonances and their coalescence. The resonances marked by "*" correspond to CH_{phenyl} resonances.

constant may be too large for a five-bond spin−spin coupling interaction that would proceed through the naphthalene backbone. It turn, this coupling possibly reflects the presence of a direct C(02)−F interaction. In accordance with the above observations, the ^1H spectrum of $[\mathbf{1}-F]^+$ at −60 °C in $CDCl_3$ displays six distinct resonances for the naphthalene H-atoms. Upon elevation of the temperature, however, the peaks become broader and eventually coalesce (Figure 7). These results can be interpreted on the basis of a fluxional system in which the fluoride anion oscillates between the C(01) and C(02) centers (Scheme 4) with apparent activation parameters of $\Delta H^{\ddagger} = 52(\pm 3)$ kJ mol^{-1} and $\Delta S^{\ddagger} = -18(\pm 9)$ J K^{-1} mol^{-1} as derived from line shape analysis. The ^{19}F NMR resonance of the $[BF_4]^-$ anion appears at −150 ppm.[47] This chemical shift is identical to that typically observed for free $[BF_4]^-$ anion. Moreover, this resonance does not change as a function of temperature, thus

(41) Further details on calculated structures can be found in the Supporting Information.
(42) Bader, R. F. W. *Atoms In Molecules: A Quantum Theory*; Oxford: New York, 1990.
(43) AIM2000 − Biegler-König, F. W.; Schönbohm, J.; Bayles, D. *J. Comput. Chem.* **2001**, *22*, 545. http://www.aim2000.de/.
(44) Details of the AIM analysis including density and Laplacian values for all atomic, bond, ring, and cage critical points can be found in the Supporting Information.
(45) Boys, S. F. *Rev. Mod. Phys.* **1960**, *32*, 296. Boys, S. F. In *Quantum Theory of Atoms, Molecules, and the Solid State*; Lowdin, P. O., Ed.; Academic Press: New York, 1966; pp 253−262.
(46) Weigert, F. J. *J. Org. Chem.* **1980**, *45*, 3476.

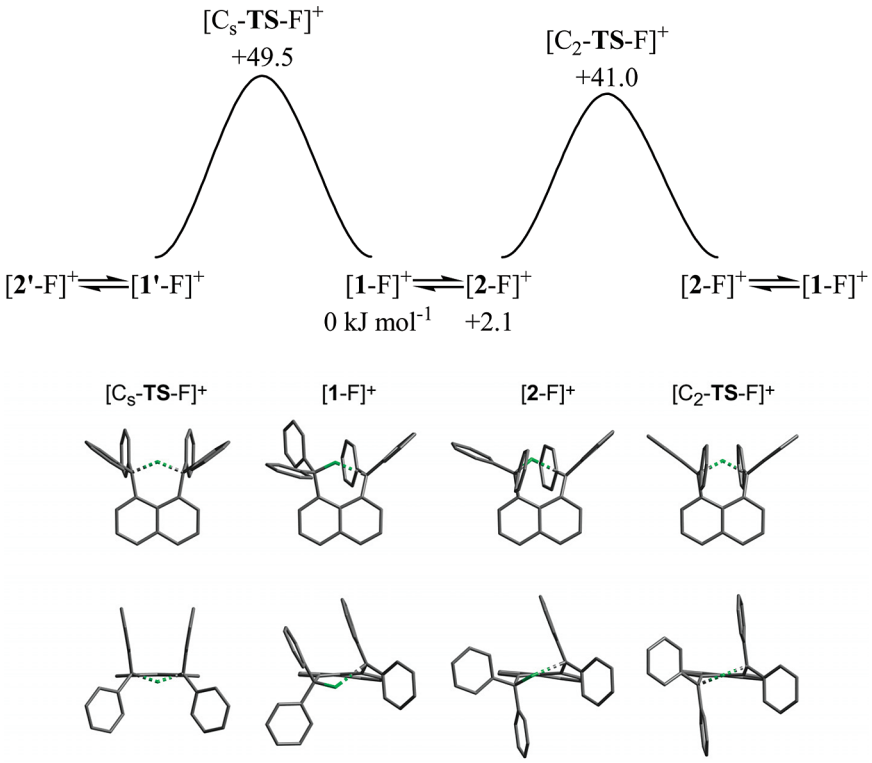

Figure 8. B3LYP calculated pathways and structures involved in the oscillation of the fluorine atom. [**1**−F]$^+$ and [**2**−F]$^+$ are two minima, and [**1′**−F]$^+$ and [**2′**−F]$^+$ are their respective enantiomers. [C_2−**TS**−F]$^+$ and [C_s−**TS**−F]$^+$ are two transition states. The low-energy transition state ([$\mathbf{TS_{1-2}}$−F]$^+$) connecting [**1**−F]$^+$ and [**2**−F]$^+$ is not pictured. The structures of the four stationary points on the PES ([**1**−F]$^+$, [**2**−F]$^+$, [C_2−**TS**−F]$^+$, and [C_s−**TS**−F]$^+$) are presented in two views, one parallel to the naphthalene ring and a second perpendicular to the naphthalene ring. MP2 structures and energies are very similar, see text.[48]

Scheme 4

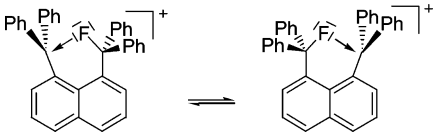

indicating that the [BF_4]$^-$ anion is not involved in the observed dynamic process.

To further investigate this exchange process, its potential energy surface (PES) was explored with B3LYP and MP2 methods. The energies given are enthalpies. Calculations of the geometries and relative energies of various stationary points on the PES indicated the presence of a second C_1 minimum [**2**−F]$^+$ which resides only 2.2 kJ mol^{-1} (B3LYP) and 12.8 kJ mol^{-1} (MP2) higher than [**1**−F]$^+$. The structures of [**2**−F]$^+$ and [**1**−F]$^+$ are very similar and only differ by the respective orientation of the phenyl rings: [**1**−F]$^+$ has two phenyl rings π-stacked approximately eclipsing each other; [**2**−F]$^+$ has two sets of two phenyl rings interacting edge to face (Figure 8). (A low-energy transition state connects [**1**−F]$^+$ and [**2**−F]$^+$, vide infra.) Two transition states for the fluorine transfer were also located. Both of these transition states, [C_2−**TS**−F]$^+$ and [C_s−**TS**−F]$^+$, feature a symmetrically bridging fluorine atom and can be described as symmetric fluoronium ions. Analytical frequency calculations confirm both are true transition states because both [C_2−**TS**−F]$^+$ and [C_s−**TS**−F]$^+$ have one and only one imaginary frequency (first-order saddle points on the PES). The geometry of both transition states merits comment. The symmetrically coordinated divalent fluorine atom forms two equivalent C−F bonds of 1.763 Å ([C_2−**TS**−F]$^+$) and 1.752 Å ([C_s−**TS**−F]$^+$) and a C−F−C angle of 126.3° ([C_2−**TS**−F]$^+$) and 124.6° ([C_s−**TS**−F]$^+$) which differ markedly from the situation observed or calculated for [**1**−F]$^+$ or calculated for [**2**−F]$^+$ (Table 2).

The low-energy transition state ([$\mathbf{TS_{1-2}}$−F]$^+$ not pictured) at +6.5 kJ mol^{-1} (B3LYP) and +17.3 kJ mol^{-1} (MP2) as compared to [**1**−F]$^+$ connects [**1**−F]$^+$ and [**2**−F]$^+$, and both [**1**−F]$^+$ and [**2**−F]$^+$ exist as two enantiomers. Therefore, four low-energy species exist, and all persist even at low temperatures (Figure 8). The fluorine transfer process originating from [**1**−F]$^+$ occurs through [C_s−**TS**−F]$^+$ and produces the other enantiomer, [**1′**−F]$^+$. The fluorine transfer process originating from [**2**−F]$^+$ occurs through [C_2−**TS**−F]$^+$; it does not lead to an inversion of the conformation and produces the same enantiomer, [**2**−F]$^+$. The calculated activation parameters of $\Delta H^{\ddagger} = 41.0$ kJ mol^{-1} and $\Delta S^{\ddagger} = 2.4$ J mol^{-1} K^{-1} for [C_2−**TS**−F]$^+$ and $\Delta H^{\ddagger} = 49.5$ kJ mol^{-1} and $\Delta S^{\ddagger} = 29.4$ J mol^{-1} K^{-1} for [C_s−**TS**−F]$^+$ (DFT-B3LYP) are in reasonable agreement with those determined experimentally ($\Delta H^{\ddagger} = 52(\pm3)$ kJ mol^{-1} and $\Delta S^{\ddagger} = -18(\pm9)$ J mol^{-1} K^{-1}). Møller Plesset second-order perturbation theory (MP2) produces similar barriers, $\Delta H^{\ddagger} = 50.3$ kJ mol^{-1} for [C_2−**TS**−F]$^+$ and $\Delta H^{\ddagger} = 55.8$ kJ mol^{-1} for [C_s−**TS**−F]$^+$. In light of these theoretical findings, it can be concluded that the low-

(47) Drago, R. S. In *Physical Methods For Chemists*, 2nd ed.; Surfside Scientific Publishers: Gainesville, FL, 1992; p 235.
(48) JIMP and POV-Ray 3.5 were used in the production of Figure 8. Manson, J.; Webster, C. E.; Hall, M. B. JIMP Development Version 0.1 (built for Windows PC and Redhat Linux 7.3), March 2003; Department of Chemistry, Texas A&M University, College Station, TX 77842. http://www.chem.tamu.edu/jimp/.

Scheme 5. Resonance of the Canonical Representations of $[\mathbf{1}-F]^+$

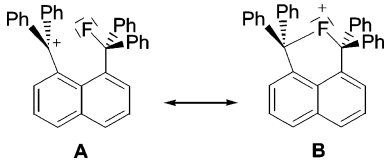

temperature NMR spectrum recorded at −60 °C most likely corresponds to the averaged spectra of $[\mathbf{1}-F]^+$ and $[\mathbf{2}-F]^+$ which even at this temperature are in rapid equilibrium. Because the calculations show that the path for the higher $\Delta H^{\ddagger}$ has the larger $\Delta S^{\ddagger}$, this higher-energy path will contribute more to the rate as the temperature is raised and will cause the experimental analysis which assumes a single path to produce an intermediate value for $\Delta H^{\ddagger}$.

Concluding Remarks

The structure of $[\mathbf{1}-F]^+$ can be largely accounted for by considering the methylium description **A** (Scheme 5) which is supported by the approximate trigonal planar arrangement of the C(02) carbon atom as well as its ^{13}C NMR chemical of 209.3 ppm (Scheme 5). However, by virtue of the bonding interaction between C(02) and F, which is supported by both experiment and theory, the unsymmetrical fluoronium description **B** (Scheme 5) must also be contributing. The variable-temperature solution studies of this ion allow us to witness the oscillation of a fluorine atom between two carbon centers on the NMR time scale. Taking into account the strength of the carbon−fluorine bond and its chemical inertness, the occurrence of this transfer process, which involves the concomitant lengthening and shortening of a C−F bond, is rather unusual and suggests that cationic pathways are available for the activation of primary C−F bonds. This assertion corroborates the finding of Lectka and co-workers who have proposed the formation of a fluoronium intermediate in the intramolecular reaction of a carbocation with a C−F bond.[7] The fluxionality of the structure of $[\mathbf{1}-F]^+$ also indicates that symmetrical fluoronium ion species constitute low-energy transition states for such processes. These results are of possible relevance to C−F bond activation chemistry, an area that has witnessed a spur of interest[49] caused by the environmental accumulation and nuisance of fluorocarbons.[50−53]

Acknowledgment. This paper is dedicated to Alan H. Cowley on the occasion of his 70th birthday. This work was supported by the National Science Foundation (CHE 00-94264, Career Award to F.P.G.; CHE 98-00184 and 02-16275, support for computational calculations; CHE 98-07975, purchase of the X-ray diffractometers; and CHE 00-77917, purchase of NMR instrumentation) and the Welch Foundation (A-648). We also thank the Laboratory for Molecular Simulation at Texas A&M University for providing computational software and computing time.

Supporting Information Available: Spectroscopic and crystallographic data (CIF), as well as further computational details. This material is available free of charge via the Internet at http://pubs.acs.org.

JA048501Y

(49) Mazurek, U.; Schwarz, H. *Chem. Commun.* **2003**, 1321. Kiplinger, J. L.; Richmond, T. G.; Osterberg, C. E. *Chem. Rev.* **1994**, *94*, 373.
(50) Ravishankara, A. R.; Solomon, S.; Turnipseed, A. A.; Warren, R. F. *Science* **1993**, *259*, 194.
(51) Lemal, D. M. *J. Org. Chem.* **2004**, *69*, 1.
(52) Tsai, W. T.; Chen, H. P.; Hsien, W. Y. *J. Loss Prev. Process Ind.* **2002**, *15*, 65.
(53) Khalil, M. A. K.; Rasmussen, R. A.; Culbertson, J. A.; Prins, J. M.; Grimsrud, E. P.; Shearer, M. J. *Environ. Sci. Technol.* **2003**, *37*, 4358.